DEVELOPMENT AND EXPERIMENTAL VALIDATION OF A FULLY-ELECTRODELESS ELECTRIC PROPULSION SYSTEM FOR SATELLITE OPERATIONS IN LOW EARTH ORBIT

Anna-Maria Theodora ANDREESCU[1,2], Daniel Eugeniu CRUNTEANU[2], Simona DANESCU[1], Maximilian Vlad TEODORESCU[3], Adrian STOICESCU[1], Alexandru CANCESCU[1]

This paper presents the design, fabrication, and experimental validation of disruptive Electric Propulsion (EP) system. The system features a compact helicon reactor integrated with a multi-dipole cusp magnetic confinement system, aligning with the emerging trends in the Low Earth Orbit (LEO) propulsion sector. This approach aims to meet the increasing demands for efficient, compact, and sustainable propulsion solutions suitable for modern satellite missions. This research aims to enhance the throttleability of a compact Helicon Plasma Thruster (HPT) by managing ion energies via transitions from Capacitive Coupled Plasma (CCP) modes to Inductive Coupled Plasma (ICP) modes. This was achieved by adjusting the RF input power while maintaining a constant magnetic field. Through the experimental testing campaign, it has been proved the jump power threshold of the CCP-ICP at 200 W for an argon flow rate of 8 standard cubic centimeter per minute (sccm) by means of Optical Emission Spectroscopy. The findings provide guidelines for further optimization of the HPT, aiming to achieve a comprehensive understanding of the argon plasma structure inside a compact magnetically enhanced inductively reactor.

Keywords: helicon waves, capacitive coupled plasma, inductively coupled plasma, throttleability, multi-mode helicon reactor

1. Background and motivation

The global space propulsion market is forecasted to expand significantly in the upcoming years, fuelled by a marked increase in space exploration activities. This growth is further supported by advancements in technology miniaturization and extensive experience in design, which are collectively broadening access to space.

To surmount the limitations inherent in current in-space propulsion technologies, it is essential to innovate and develop new systems that align with the requirements of future space missions. Emerging technologies like cathodeless

[1] Romanian Research & Development Institute for Gas Turbines COMOTI, Romania, email: theodora.andreescu@comoti.ro
[2] National University of Science and Technology POLITEHNICA Bucharest, Faculty of Aerospace Engineering , Romania
[3] Romanian Space Science Institute, Magurele, Romania

plasma thrusters are at the forefront of this innovation, offering key advantages such as enhanced reliability, adjustable throttle control, extended operational lifetime, and reductions in both initial development and ongoing operational costs [1-11] These improvements are critical for advancing the capabilities of propulsion systems in the context of evolving demands in space exploration and satellite deployment.

This paper explores the mechanism of helicon plasma production, addressing several critical physical issues with the strategic aim of advancing the development of a wave-heated Electric Propulsion system. Designed to achieve variable thrust with a specific impulse exceeding 1000 seconds, the HPT is a highly efficient solution for contemporary space propulsion needs. A pivotal aspect of the electrodeless Helicon Plasma Thruster (HPT) concept lies in the development of an ultra-compact annular helicon plasma source. This reactor must effectively interface with an acceleration stage, represented by a magnetic nozzle, to facilitate efficient plasma propulsion.

Several research teams globally have successfully developed Helicon Plasma Thrusters (HPTs). Advanced Concepts such as Variable Specific Impulse Magnetoplasma Rocket (VASIMR) [2-3] and others Helicon Double Layer Thruster –HDLT (~1kW,~11mN) [4-6], Mini-helicon Plasma Thruster (~1kW,~11mN) [7] are in various stage of development and field test, offering a great promise for the future of space exploration.

The operation of micro-satellites in low Earth orbits (LEO) faces several challenges, including limited maneuverability, uncertainty in end-of-life disposal, and a reduced operational lifespan caused by atmospheric drag and the rapid degradation of conventional propulsion systems due to the presence of residual atmospheric gases. This paper aims to extend the commercial incentives of small satellite buses in the 200 to 500 kg mass range at low altitudes by enabling precise low-thrust orbital control and maneuvering within the millinewton range. To achieve this goal, this study evaluates a disruptive EP technology and explores the operability of its plasma source during the transition from capacitive coupled mode to inductive coupled mode. The helicon-plasma heating technique applied to space propulsion systems enables operation across a broad range of thrust levels by merely adjusting the propellant flow rate or the RF input power within the discharge chamber. This electrodeless ionization method provides throttling capabilities for precise thrust adjustments, ensures minimal propellant consumption, and enhances maneuverability and mission versatility, all of which are crucial to meeting the dynamic demands of modern space exploration.

Furthermore, the availability of small, throttleable thrust can enhance the effectiveness of attitude control functions, such as asymmetric torque compensation, which reduces the need for frequent desaturation maneuvers and ultimately leads to smoother control. Several key factors arise from the LEO space

flight, such as low mass and power consumption, high specific impulse and low thrust levels, high modularity, low development cost and ease of interface with small-satellite buses. Table 1 outlines the initial performance objectives for the LPHPT family.

Table 1

Preliminary LPHPTs operational envelope

Preliminary Performances	**Value**
Specific impulse	>1000s
Power consumption	<50 W⁄mN
Thrust levels	2 to 10 mN
Throttleability range	40% to 120% of nominal thrust
Mass including power input	<0.6 kg/mN

This paper explores comprehensively the discharge characteristics of both Capacitive Coupled Plasma (CCP) and Inductive Coupled Plasma (ICP) excited mode within the same helicon source, specifically designed for space propulsion applications. Section 2 introduces the breakthrough in Helicon Plasma Thruster principle of operation. Section 3 describes the characteristics of the vacuum experimental set-up and diagnostics for E to H mode transition. Section 4 provides a preliminary measurement results for the argon plasma operating in a Continuous Wave mode up to 200 W RF input power.

2. The basic physics of helicon plasma thrusters

The HPT integrates features of a two-stage, magnetically enhanced inductively coupled plasma source: dense plasma generation within the discharge chamber and supersonic acceleration of quasi-neutral plasma plume in the magnetic nozzle. In this advanced space transportation concept, the propellant is ionized by resonant excitation of helicon waves. Helicon are long-wavelength electromagnetic waves that operate within frequency ranges spanning from the lower-hybrid frequency to the electron cyclotron frequency in magnetized plasmas [12]. These waves are often referred as high-frequency compressional Alfven waves or low-frequency whistlers.

While whistler waves exhibit characteristics of right-hand circularly-polarized electromagnetic waves in free space, their confinement within a radially-bounded medium introduces an electrostatic component that aligns longitudinally along the magnetic field lines, transforming them into waveguide modes known as helicons [13,14]. Additionally, the system can support long-wavelength electron cyclotron waves, referred to as Trivelpiece-Gould (TG) waves [15]. TG waves are highly damped, enabling them to penetrate the core of the plasma reactor at lower magnetic field strengths. Conversely, at higher magnetic field strengths, they are capable of depositing significant power at the plasma's edges. Thus, in a HPT based on azimuthally asymmetric antenna, the excited fields can be interpreted as a superposition of both Helicon and TG waves, each contributing distinctively to the

plasma dynamics within the reactor [16]. TG waves results from the constructive interference [17,18] that occurs when the resonance cones of whistler waves are reflected off the physical boundaries of the reactor. This interaction is a key dynamic within the reactor, influencing the wave patterns and their effects within the plasma environment.

In the second stage, several critical processes can be identified, including supersonic acceleration, thrust transmission, plasma detachment, and the formation of a double layer. The MN is entrusted with transforming the thermal energy of the plasma into directed kinetic energy of ions. Electrons being fully magnetized at 800 G while ions being weakly magnetised at this field range, in their outwardly expansion will induce an ambipolar electric field to preserve the quasi-neutrality of the RF plasma [6]. Under these conditions, the applied and induced fields interact repulsively, producing the magnetic thrust. During the acceleration phase, the electric potential drop across the system is proportional to the electron temperature. As the field lines within the magnetic nozzle begin to diverge, there is a corresponding decrease in plasma density, both axially and radially. This decrease facilitates the demagnetization of both electrons and ions, allowing them to detach from the magnetic field lines [8].

The schematic diagram of the system based on magnetically enhanced inductively coupled plasma (MEICP) involved in the experimental testing campaign is presented in Figure 1. The HPT breadboard model features a quartz discharge chamber with an outer diameter of 30 mm and a length of 150 mm. In terms of wave generation it features an azimuthally asymmetric half-wavelength right helical (HWRH antenna), measuring 78 mm in length and 1.25 mm in thickness, wrapped around the reactor`s walls. Additionally, to ensure the optimal environment for efficient wave-plasma energy deposition, the HPT engineering prototype incorporates a multi-dipole magnetic confinement system based on eight plate-shaped NeFeB permanent magnets of 38 EH grade, each gold-plated, measuring 70 mm in length, 10 mm in width, and 5 mm in thickness. These magnets are configured in alternating rows of north and south poles along the confinement tube, capable of producing a magnetic field strength of 800 Gauss. For plasma acceleration, the design includes a ring-shaped NdFeB 38EH grade permanent magnet strategically positioned in the throat section of the HPT.

In the current Electric Propulsion (EP) system, a HWRH antenna is utilized, specifically designed to heat the plasma through stochastic interactions between RF energy and electrons [19]. The antenna emits a time-varying magnetic field along its length, which effectively couples with the transverse magnetic field characteristic of the helicon mode [17,19,20].

When powered by an RF generator, the HWRH antenna induces an azimuthal sinusoidal distribution of oscillating currents within its structure,

enabling resonance near the frequency of 13.56 MHz, and ionizing argon neutral gas immersed in the magnetosonic field.

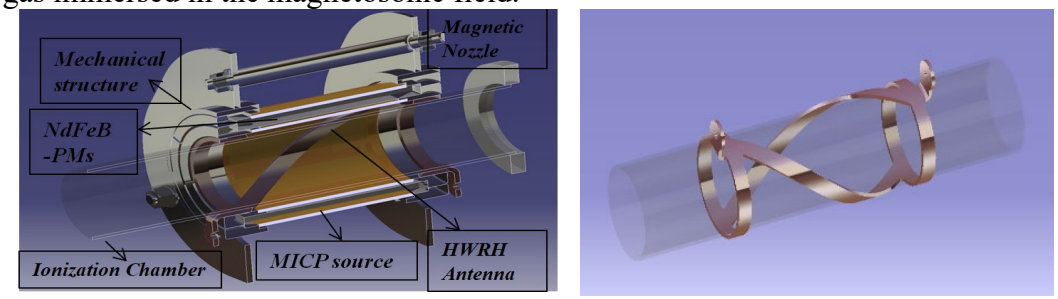

a) b)

Fig. 1. a) Helicon Plasma Thruster CAD sketch; b) azimuthally asymmetric Half-wavelength Right Helicon

To facilitate impedance matching between the RF Generator and the antenna/plasma system, a Variable Matching Network (VMN) should be employed. This capacitor control box adjusts the impedance of the m=+1 mode antenna to the 50Ω output of the RF Generator, ensuring efficient power transfer and minimizing losses. This HPT is designed according to helicon cold wave theory and global model (GM) of particle and power balance.

The GM [12] was involved to determine the plasma density, plasma potential and electron temperature inside the MEICP source. The particle balance equation predicts electron temperature by equating the total surface particle loss to the total volume ionization:

$$n_0 u_B (2\pi R_s L_s h_R + 2\pi R_s^2 h_L) = K_{iz} n_g n_0 \pi R^2 L_s, \quad (1)$$

with h_R, h_L representing the radial and axial sheath edge, K_{iz} ionization rate coefficient, n_0 the bulk density, n_g the argon neutrals density, $u_B = \sqrt{kT_e/m_i}$ the Bohm velocity, R_s, L_s radius and length of the ionization chamber.

The axial sheath edge is defined by Equation 2:

$$h_L = 0.86\left(3 + \frac{L_s}{2\lambda_i}\right)^{-1/2} = 0.486 \quad (2)$$

Due to the magnetic confinement, the radial sheath edge becomes zero:

$$h_R = 0.80\left(4 + \frac{R_s}{\lambda_i}\right)^{-1/2} = 0 \quad (3)$$

The effective plasma size for particle loss is:

$$d_{eff} = \frac{1}{2}\frac{R_s L_s}{R_s h_l + L_s h_R} = 15.413\ cm, \quad (4)$$

The electron temperature was determined based on the effective plasma size $n_g d_{eff} = 3.08 \cdot 10^{18}\ (m^{-2})$, resulting in T_e~3.9eV,

The core plasma density n_0 could be determined from energy balance by equating the total absorbed power to the total power lost [12]:

$$n_0 = \frac{P_{abs}}{eu_B A_{eff} \mathcal{E}_T} = 2.4 \cdot 10^{13} cm^{-3} \quad (5)$$

with the effective particle loss area defines by:

$$A_{eff} = 2\pi R_S^2 h_L + 2\pi R_S L_S h_R = 6.875\ cm^2 \quad (6)$$

When axial magnetic field is $400G$ and using an expected plasma density of approximately $2.4 \cdot 10^{13} cm^{-3}$ with an RF frequency of $13.56\ MHz$, the axial wavelength is:

$$\lambda_z = \frac{3.83 B_0}{R_s n_0 e \mu_0 \omega} = 15.64\ cm \quad (7)$$

The size of the HWRH antenna was determined by assuming a resonance mechanism with the nominal wave (NW) mode, propagating in the magnetized plasma. This resonance is respected when the parallel wavelength is twice of the nominal length:

$$L_{HWRH} = \frac{\lambda_z}{2} = 7.8\ cm \quad (8)$$

From Equation (7) it can be observed that both the $\boldsymbol{B_0}$ and $\boldsymbol{n_0}$ define the axial wavelength of helicons. The external magnetic field should be selected carefully, as exceeding a certain threshold can lead to a decrease in plasma density. This reduction in density can have adverse effects on the propulsion metrics of the thruster, potentially compromising its performance and efficiency. The decrease in plasma density beyond a certain magnetic field threshold can be explained by considering the impact of low-frequency electrostatic instabilities [21-23]. These instabilities can lead to increased radial diffusion, which disrupts plasma equilibrium. Specifically, this radial diffusion is often induced by resistive drift-wave instability, driven by gradients in plasma pressure and density, as well as by Kelvin-Helmholtz instabilities [24]. M. Light et al. [21,25]experimentally validated this theory, providing empirical evidence for the existence and impact of such instabilities on plasma behavior.

3. **Experimental platform and diagnostic method**

During the experimental testing campaign, the HPT experimental prototype is placed within a cylindrical vacuum chamber equipped with multiple diagnostic ports, as shown in Figure 2.a. The chamber, measuring 400 mm in length and 508 mm in inner diameter, is equipped with several flanges that provide electrical, gas, and optical feedthroughs. It also features a DN 159 gate valve, which facilitates the connection to the pumping system. The chamber is constructed from nonmagnetic stainless steel, chosen for its resistance to deformation under high-vacuum conditions. This design ensures the chamber can effectively replicate the environmental conditions of outer space. Ultrahigh-purity (99,999%pure) Argon propellant is supplied to the vacuum side through a Bronkhorst volumetric flow controller, model EL-FLOW F-201CV-500-AGD-33-V, with an accuracy of 0.1

sccm, being calibrated to supply between 5 and 500 sccm full range. The pumping system is based on two different vacuum technologies: a dry mechanical Pfeiffer pump ACP 28-40 and a turbo-molecular Pfeiffer pump (HiPace® 400 with a TC 400 controller). A valve with manual actuator is installed between the mechanical pump and the turbomolecular pump to prevent back flow. Measurements of this magnetic field were carried out using an FM 302 teslameter equipped with a calibrated AS-NTM probe, ensuring accurate and reliable data collection for the system's performance evaluation.

The experimental testing platform during the commissioning procedure is depicted in Figure 2.b. The HPT breadboard model is powered by a specifically designed RF system comprising a custom-off-the-shelve RF Generator (Coaxial Power – RFG600-13) and a Matching Box (AMN600).

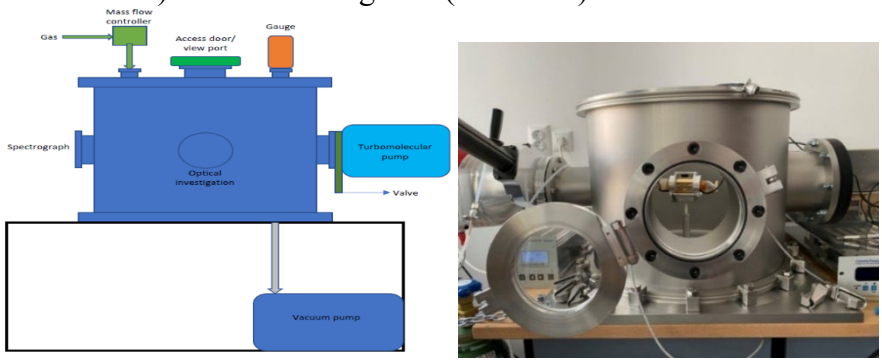

a) *b)*

Fig.2 a) Schematic representation of the experimental testing platform , b) Representative picture of the HPT`s commissioning procedure

The HPT breadboard model is powered by a specifically designed RF system comprising a custom-off-the-shelve RF Generator (Coaxial Power – RFG600-13) and a Matching Box (AMN600). This system includes an L-type capacitor control box that ensures power transfer maximization. These capacitors allow for manual adjustments to achieve optimal impedance matching when the automatic mode does not provide satisfactory results. The RF generator is capable of delivering up to 600 W of RF power, with a maximum allowable reflection power of 90W and is designed with an inbuilt standard output resistance of 50 Ω.

To highlight the E-H mode transition through non-intrusive methods, an Optical Emission Spectroscope (AvaSpec-ULS4096CL-EVO) with wavelength ranging from 200 to 1100 nm was involved, with an averaged spectral resolution of 0.1 nm. Wavelengths of emission lines and their excitation energies were systematically compared with entries in the NIST Atomic Spectra Database Lines. This comparison was conducted to ensure that the measurements conformed to international standards, providing validation and credibility to the spectral data obtained during the experiments [26].

4. Experimental testing campaign

To assess readiness of the LPHPT operating in continuous wave mode (CWM), a comprehensive test plan has been proposed. This program includes an ignition procedure and maiden test to determine nominal propellant feed rates, followed by steady – state operation across different RF power envelopes with plasma heating for up to 60 minutes to assess the thrust`s thermal response. Additionally, unsteady-state characterization during the E to W mode transition was proposed by local OES, with the strategic goal to ensure a synergistic correlation between the plasma parameters and the HPT propulsion metrics. For comparative analysis, the emission intensities of the ArII ion lines at 480.6 nm and 434.8 nm, as well as the ArI atom line at 811.3 nm and 750.4 nm, were measured as the RF power was progressively increased from 50 W to 200W. Table 2 provide a summary of the operating parameters for the LP-HPT experimental prototype.

Table 2

The operating parameters for the LP-HPT proof-of-concept

Operating parameter	Value
RF Power Envelope	50 – 200 W
Argon fill pressure	1 mTorr
Mass flow rate	8 sccm
Driving frequency	13.56 MHz
Magnetic field at the HWRH antenna	400G
Magnetic field at the MN section	800G
Magnetic field direction	Downstream
Axial helicon wavelength	15.64 cm
Spectrometer axial position	At the magnetic nozzle critical section

During the spectral measurement procedure, after the background pressure within the vacuum chamber was stabilized around $2 \cdot 10^{-5}\ mbar$ the argon was injected into the HPT through a cooper pipe as a gas flow line. Second, the RF Generator and the Matching Network were triggered on. It was determined that the optimal propellant flow rate for operations in Continuous Wave (CW) mode is 8 standard sccm. This value was identified as providing the best balance between efficiency and performance under the specified operational conditions. To evaluate the capacitive (E) to inductive (H) transition, the RF energy was varied from 8W to 200 W The thruster started to ignite at 8W forwarded power (P_{wd}), at an argon mass flow rate of 6 sccm (Figure 3). In the continuous wave mode testing scheme, the argon propellant flow rate was increased from 6 standard cubic centimetres per minute to 8 sccm after the first ignition test sequence, underlined in Figure 3. The rise in neutral flow rate was coordinated with an increase in RF energy, reaching up to 50 W (Figure 4). The representative emission spectrum of argon helicon plasma in the E- mode of operation is depicted in Figure 5, where the strongest low-energy electron excited neutral lines are Ar I 811.3 nm, Ar I 772.3 nm, Ar I 763.5 nm and Ar I 750.4 nm, having the excitation energy of $13.07eV$, $13.15eV$, $13.17eV$

and 13.47 eV. In CCP operation, the emissions of Ar atom line, ranging from 700 to 900 nm are dominant.The red-pink core of the plasma discharge, characterized by the argon ion emission lines around 480.6 nm and 488 nm, exhibits consistent brightness throughout the ionization chamber.

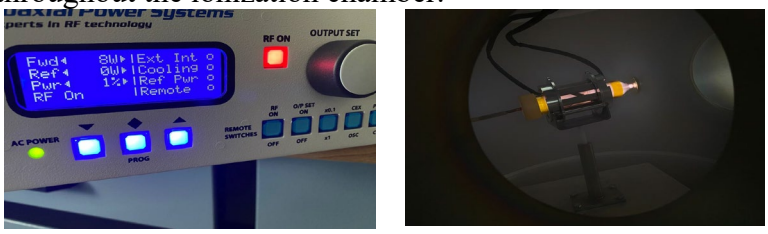

a) b)

Fig. 3 a) Capture from the RF generator, highlighting the main power outputs;b) HPT operating in CW mode with 6 sccm of Argon and 8W forwarded power

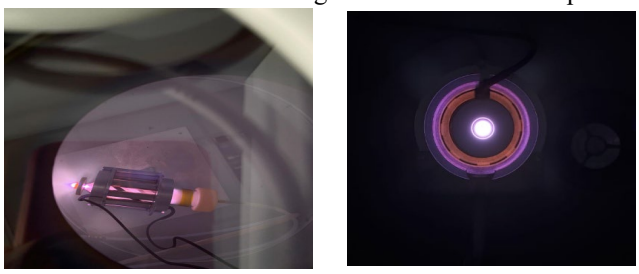

a) b)

Fig.4 a) Top view of the HPT experimental prototype in CWM operation under 8 sccm of Argon and 50 W forwarded power; b) HPT plume plasma structure

Notably, an intensified pink glow is observed in the critical section of the magnetic nozzle, primarily due to the acceleration of plasma flow ions through the ambipolar potential drop. In this region, interactions between populations of electrons and ions occur, maintaining a quasi-neutral electric charge.

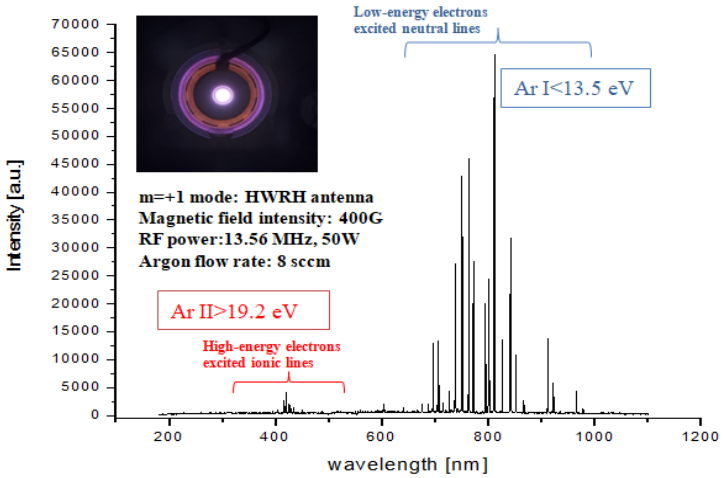

Fig.5 Optical emission spectra and photograph of plasma plume in 8 sccm of argon at 50 W Capacitively Coupled Mode

To determine the electron temperature (T_e) in argon MEIC plasma, the emission line ratio method of Ar I 811.3 nm and 750.4 nm based on OES was selected to simplify the balance equations of collisional radiative model (CRM). Ar I 811.3 nm and 750.4 nm in current breadboard model are excited due to direct ground-state excitation collision and the metastable atom excitation collision. Furthermore, since the density of metastable argon is correlated with both the electrons and neutral ground-state argon atoms, the rate coefficients described by the CRM model can be considered as functions of the electron temperature. Considering that the electrons follow a Maxwellian distribution, at a working pressure of $3.9 \cdot 10^{-3}\, mbar$, the resulting electron temperature for the 50 W forwarded power, with a reflected power of 8W, was determined to be 3 eV, based on the theoretical $I_{811.3nm}/I_{750.4nm}$ ratio. This result is consistent with the global model discussed in Section 2.

As the RF power input in the HPT was progressively increased from 50 W to 200 W, the discharge inside the MEICP source ramp up from CCP to ICP mode. The result of inductively coupled plasma operation (H-mode) is underlined in Figure 6. It was observed that positioning the propellant feed near the magnetic nozzle enhances wave-plasma coupling and promotes favourable collimation of the argon plasma plume. This improvement is attributed to the reduction of losses caused by the interaction of charged particles with the chamber walls. The spectral curve after the H mode jump underlines the fact that 700-900 nm Ar atoms cluster is the significant one, being presented in Figure 7. Similar to the E mode of operation, the electron temperature is determined from the ratio of argon emission lines 811.3 nm ($2p_9 \rightarrow 1s_5$) and 750.4 nm($2p_1 \rightarrow 1s_2$). The intensity ratio $I_{811.3nm}/I_{750.4nm}$ yields a value of 1.13, corresponding to a relatively high electron temperature of 5.5 eV.

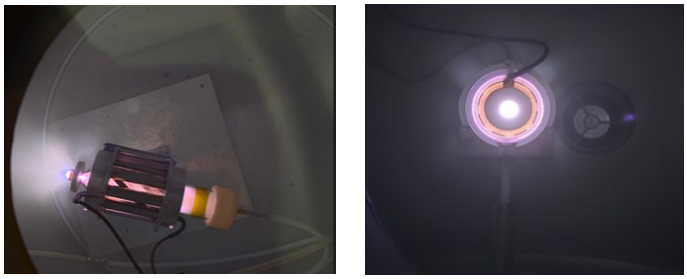

a) b)

Fig.6 a) Top view of the HPT experimental prototype in CWM operation under 8 sccm of Argon and 200 W forwarded power; b) HPT plume plasma structure

The emission intensity of atom lines (ArI) decreases in H mode due to neutral depletion mechanism. On the other hand, the ion lines exhibit a weak signal; however, their intensity shows a slight increase as the RF power is raised. During the E-H mode transition, the growth rates of the high-energy electron-excited ionic

populations at 434.8 nm, 480.6 nm, and 488 nm increase from 728.31 a.u. to 1507.61 a.u., from 483.91 a.u. to 999.34 a.u., and from 707.38 a.u. to 1120.04 a.u., respectively. The trend in these ArII intensities is highlighted in Figures 5 and 7. The argon ion emission of 434.8 nm is a representative index of the ICP mode transition of argon helicon – heated plasma. At 200 W RF power, the core of the MEICP source takes on a faint blue hue. During the CCP and ICP modes, the stochastic electron heating region is located within the skin layer, resulting in electrons being confined near the edge by the external magnetic field. This leads to a relatively low plasma density in the centre, accompanied by weak neutral depletion, as indicated by the strong ArI emission lines. However, when the HPT mode is initiated, core heating becomes dominant, significantly increasing the ionization rate in the centre. Neutral depletion begins to occur, facilitating argon neutral heating through ion-neutral elastic collisions, electron-neutral elastic collisions, and ion-neutral charge exchange collisions. The faint blue light observed in the H mode is a spectral characteristic of MEICP sources, reflecting specific spatial distributions of ion and atom line emissions. The results obtained are consistent with the findings reported by Ying et al. [27], who successfully achieved H-mode coupling using an RF input power of 180 watts at a frequency of 13.56 MHz, operating with argon. Their setup involved a helicon plasma source with a 50 mm outlet diameter, which utilized two sets of ring array permanent magnets to facilitate the process.

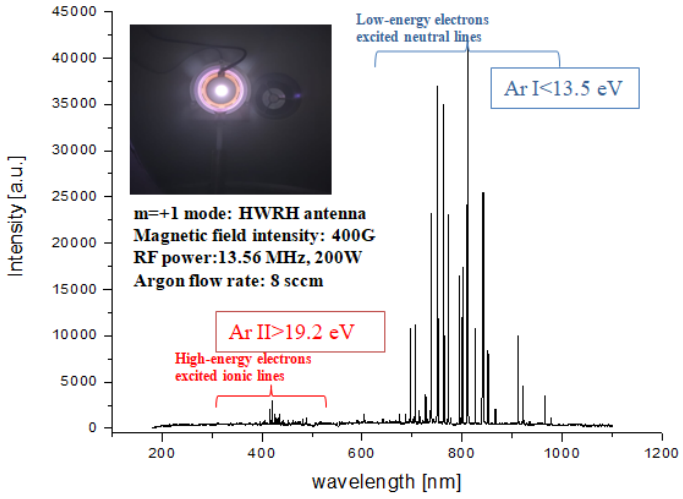

Fig.7 Emission spectra and plasma plume image at 200 W continuous RF wave energy

In space electric propulsion (EP) systems, the ion energy distribution along the magnetic nozzle is crucial, as it is a primary factor contributing to effective thrust generation. Due to the influence of the magnetic nozzle, an electric double-layer structure forms downstream of the Helicon Plasma Thruster's critical section,

marked by a sharp potential gradient. This structure results in a reduction of plasma density by a factor of approximately$exp(-1/2)\sim0.61$, resulting in supersonic ion beam. The Bohm velocity $C_s = (eT_e/M_i)^{1/2}$was determined for the 50 W and 200 W power thresholds. In the CCP mode, with an electron temperature of$T_e\sim3\ eV$, considering the argon ion mass $M_i = 1.67 \cdot 10^{-27} kg,$ the ion sound speed is approximately $C_s \cong 2680\ m/s$. In contrast, in the ICP mode, with$T_e\sim5.5\ eV$, the corresponding Bohm velocity is $C_s \cong 3629.5\ m/s$. The beam velocity of the HPT plasma plume was correlated with the double-layer formation by taking into account an acceleration coefficient α equal to 4. Under ambipolar potential drop, the ideal specific impulse and thrust force can be expressed as $I_{sideal} = \alpha C_s/g_0$ and $T_{ideal} = I_{sideal}\dot{m}_{argon}g_0$.The resulted propulsion metrics of the HPT under 50-200 W power envelope is presented in Table 3.

Table 3

Representation of the HPT propulsion metrics in both E and H modes

Gas	RF Power (W)	Volumetric Flow Rate (sccm)	Specific Impulse (s)	Potential thrust force (mN)	F/P_{RF} (mN/kW)
Ar	50	8	1148	2.25	45
Ar	250	8	1554	3.04	15.2

The transition from E-mode to H-mode in magnetically enhanced inductively coupled plasma is a critical process that significantly enhances electron temperatures and power deposition efficiency. Understanding and controlling this transition is essential for optimizing electrodeless EO systems in the milli-Newtons thrust range. The synergistic correlation between RF input power, magnetic field strength, operating frequency and electrostatic effects governs this transition, enabling the design of more compact MEICP sources. Through a preliminary evaluation of the HPT using broadband optical spectroscopy, it has been concluded that the proposed helicon-heating technology represents a promising EP candidate, offering advanced features such as high specific impulses, low-thrust levels, throttleability, low power consumption, design modularity.

5. Conclusions

The development and testing of a groundbreaking low-power HPT intended for orbital control and manoeuvring of commercial LEO small-satellite buses have been accomplished.The drag compensation and fine trimming of orbital parameters imposes a quasi-continuous application of low thrusts and the achievement of the velocity increment over time.The main purpose of paper was to identify the nature of the inductively coupled magnetized waves with classical wave theory and to identify potential wave contribution to the plasma generation for space propulsion applications.

This paper primarily focused on describing and distinguishing the differences in LP-HPT discharge states by analysing the variations in electron temperature. Based on these changes, the thrust and specific impulse were indirectly determined. The objective was to offer a thorough understanding of how each discharge state influences the thruster's overall performance and characteristics. Given its high specific impulse capabilities and low-thrust range, the proposed HPT is well-suited for long-duration LEO missions, including tasks such as fine-tuning orbital parameters, station keeping, drag compensation, and attitude control.

The streamlined design results in a lighter EP system that is not subject to sputtering, thereby extending its operational lifespan. The reduced propellant consumption rate and the compact helicon source are key advantages for micro-satellite designs, where mass and volume constraints are of paramount importance.It was proved that ion energies in a compact helicon plasma source can be modulated by adjusting the RF power while maintaining a constant magnetic field, positioning it as a potentially disruptive electric propulsion technology for future space applications.

Acknowledgements

This work was supported by the ESA GSTP-De Risk Program under Contract No. 4000130736/20/NL/BJ/va., HEMIS-Assessments to Prepare and De-Risk Technology Developments/Helicon Plasma Thruster

R E F E R E N C E S

[1] *Mercedes Ruiz, Gomez, V. et* al.(2020). HIPATIA: A project for the development of the Helicon Plasma Thruster and its associated technologies to intermediate –high TRLs. International Aeronautical Congress (IAC) -20-C4.5.12.

[2] *Squire, J.P., Cassady, L.D., et* al.(2009).Superconducting 200kW VASIMR Experimental and Integrated Tesing.31st International Electric Propulsion Conference, IECP-2009-209.

[3] *Squire, J.P., Olsen, C.S., Frankline.R, Diaz,C. Cassedy, L.D., et al*.(2011).VASIMR VX 200 Operation at 200kW and Plume Meaurement: Future Plans and ISS EP Test Platform.32nd International Electric Propulsion Conference, IECP-2011-154.

[4] *West, M. D., Charles C. & Boswell, R. W*. (2003). Testing a Helicon Double Layer Thruster Immersed in a Space-simulation Chamber. J. Propul. Power, 24 , pp. 134-14.

[5] *Charles, C., Alexander, P., Costa, C., Sutherland, O., Boswell, R. W., et al.*(2005). Helicon Double Layer Thrusters. 29th Int. Electric Propul.Conf., IECP-2005-290.

[6] *Musso, I., Manente, M., Carlsson, J., Giacomuzzo, C., Pavarin, D., et al*.(2007). 2D OOPIC Simulations of the Helicon Double Layer.30th International Electric Propulsion Conference, IEPC-2007-146.

[7] *Batishchev, O. V*.(2009). Minihelicon Plasma Thruster, IEEE Trans. Plasma Sci., 10,1563.

[8] *Mario, M., Jaume, M., Sentiago, C.,&Eduardo, A.*(2015). Design and development of a 1 kW class helicon antenna thruster. 34th International Electric Propulsion Conference and 6th NSAT, Japan.

[9] *Chang, L., Xinyue,H*.(2018). Coupling of RF Antennas to Large Volume Helicon Plasma. AIP Advances 8 045016.

[10] *Staab,D. et al*.(2018). AQUAJET: An Electrodeless ECR Water Thruster. Proceedings of Space Propulsion Conference, CP00359.
[11] *Eduardo, A., Mario, M.(*2014).Assessment of helicon plasma thruster technology for space missions. Space Propulsion Conference, May 19-22, Cologne(Germany).».
[12] *Michael, A.L., Allan, L.L.*(2005) Principles of Plasma Discharges and Materials Processing", Second Edition, Wiley Interscience ISBN 0-471-72001-1.
[13] *Ronald, L., Kinder, Mark, J., Kishner*. (2001). Wave propagation and power deposition in magnetically enhanced inductively coupled helicon plasma sources. Journal of Vacuum Science&Technology 19,76».
[14] *Mohsen, A.& Morteza, H*.(2017). Directional power absorption in helicon plasma source excited by a half-helix antenna. Plasma Sci.Technol. 19 105403.
[15] *FF Chen and RW Boswell,* Power coupling to helicon and Trivelpiece-Gould modes in helicon sources, Physic of Plasmas, 3(5): 1783-1793, 1996.
[16] *Shogo Isayama, Shunkiro Shinohara and Tohru Hada*, Review of Helicon High-Density Plasma: Production Mechanism and Plasma/Wave Characteristics, Plasma and Fusion Research, Volume 13, 1101014 (2018.
[17] JP Klozenberg, B McNamara abd PC Thonemann, The dispersion and attenuation of helicon waves in a uniform cylindrical plasma. Journal of Fluid Mechanics, 21(3):545-563, 1965.
[18] *RW Boswell,* Effect of boundary conditions on radial mode structure of whistlers, Journal of plasma physics, 31(2): 197-208, 1984.
[19] *Konstantin, P. Shamrai & Vladimir, B. Taranov*.(1996). Volume and surface rf power absorption in a helicon plasma source. Plasma Sources Sci. Technol.5, 474-491.
[20] *RB Boswell,* Very efficient plasma generation by whistler waves near the lower hybrid frequency, Plasma Physics and Controlled Fussion, 26(10):1147, 1984».
[21] *Max Light, Francis F Chen and P L Colestock*, Low frequency electrostatic instability in a helicon plasma, Physics of Plasmas, 8, 4675, 2001.
[22] *Francis F Chen*, Low Frequency Oscillations in Gas Discharges, Physics of Fluids, 4, 1448, 1961.
[23] *Francis F Chen,* Nonlocal Drift Modes in Cylindrical Geometry, Physics of Fluids 10, 1647-1651, 1967.
[24] *F W Perkins, D L Jassby,* Velocity Shear and Low-Frequency Plasma Instabilities, Physics of Fluids 14, 102-115, 1971.
[25] *Max Light, F F Chen and P L Colestock*, Quiescent and unstable regimes of a helicon plasma, Plasma Sources Science and Technology 11, 273, 2002.
[26] NIST: Atomic Spectra Database Lines Form. Address web: https://physics.nist.gov/PhysRefData/ASD/lines_form.html. Acced day on 15.08.2024
[27] *Ying Xia, Xin Yang, Lei Chang et al.,* Development of a compact helicon plasma source with two sets of ring array permanent magnets for for the study of a blue core plasma, Review of Scientific Instruments 94, 125110, 2023.